



TAMPING TOOLS MANUFACTURING BY OPEN MOULD FORMING

Hasan Akpolat¹, Sinan Sezek², Bünyamin Aksakal³

^{1,2}Atatürk University, Faculty of Engineering, Department of Mechanical Engineering, Erzurum/ Turkey

³Fırat University School of Civil Aviation, Department of Aircraft Maintenance and Repair Elâzığ/Turkey

Corresponding Author, Sinan Sezek, ssezek@atauni.edu.tr

Abstract: Balancing of railways is very important for transport and safety. Tamping tools, picks, are balancing tools used together with Tamping machines. The production of these tools, which are used in an average of 12000 pieces per year, is very important for the national economy. From this point of view, the moulds required for the production of compaction tools used in the correction of railways were designed and analyzed. For this purpose, a closed mould of 41Cr4 steel was designed and selected for shaping the compaction tool, and FEA was carried out. Two moulds were modelled for the body connection and shovel parts. The pressing process temperature was determined as 600 °C, and the required pressing force was determined to be 250 MPa from FE analysis to minimize the effect of temperature on the microstructure. In FE analysis, parameters such as stress, strain, temperature, and metal flow were examined, and the highest stress value in the pressing process of the sphere part was found to be approximately 705 MPa at 30% deformation, and the maximum effective plastic strain was determined as 1.88 at 70% deformation. The temperature change was 684 °C in the forming of the body part and 647 °C in the forming of the sphere part. Metal flow was recorded as 271 mm/s at a 30% deformation value, where the maximum deformation occurred, and 135 mm/s in the shaping of the sphere part. The first stage for the production of tamping tool inserts, the pressing method in closed moulds, has been completed and presented in the literature.

Keywords: Tamping tools, closed die forming, FEA, steel.

1. INTRODUCTION

Distortions occur quickly on railway line axes due to the high tonnage and high-speed trips [1]. These axis distortions increase the travel time and pose a risk for safe transportation [2]. To eliminate defects caused by axis misalignment, grading machines are used in superstructure works to correct vertical (leveling) and horizontal (dressage) defects that occur along the line axis [3]. The defects formed on the railroad are measured by measuring devices and transferred to the ALC and DRP measurement system, and the measurement values are transferred to the aggregate and clamp units on the machine to make axis adjustment [4], [5].

The clamp zone lifts the line on the vertical axis in line with the values coming from the measurement system and pulls it left and right on the horizontal axis. In order to ensure that the road lifted on the vertical axis does not fall to its original position when it is released back by the clamps, ballast compaction is performed under the sleepers with the help of picks on the aggregate unit [6]. During this process, apparatus (parts) called picks are used in the auger machines. The number of picks on the auger machines varies according to the region and machine model. The picks compact aggregate in opposite positions under the sleeper lifted by the grapple [7]. During this process, fractures and abrasions occur due to the hard ground and vibration of the picks. Abrasion causes cracks, and, due to vibration, crack progression occurs on the surface, leading to a process that eventually results in fracture. Tamping tool picks, which are not produced in our country, are supplied from abroad. Production is made by chip removal and plastic deformation methods.

Tamping tools are produced by open or closed moulds. Since this process is commercial, information is not shared. Therefore, as the first step, the design of the moulds and the production of tamping tools to be produced from these moulds are made by FE analysis. Moulds and production are time-consuming and costly. FEA is essential for saving time, money, and consumables [8], [9], [10]. The resulting model can be shaped in several stages, and the process can be done hot, warm, or cold [11], [12]. In addition, different forging processes are tried to be made more efficient with different designs [13], [14], [15]. Forging has been performed by producing moulds at different temperatures and designs to save both energy and moulds [11], [16]. The mechanical properties of the materials used are of great importance for forging. Hot forging is performed especially for alloys with high yield stress, and knowing the melting points is necessary for the production of isotropic materials by creating the appropriate grain structure [12], [17], [18]. It has been shown in studies that surface roughness and smoothness tolerances are worse in hot forging process compared to warm and cold forming in materials with high yield point [15], [19], [20],

[21]. Especially in hot forging processes, the FEA method has a great role in eliminating possible errors that may arise [8], [10].

In the literature search, it was found that auger bits are generally manufactured domestically in Sweden and China. In the research conducted, it was found that many patents and trade secrets were applied for this part. This part, which can usually be produced in 3 or 4 steps, could be produced in 2 steps in our study. Based on the information obtained from limited sources in the literature, the open mold production method was selected for this part produced in a closed mold, and the press force applied was reduced from 500 kN to 200 kN, thus avoiding both energy and material losses.

2. MATERIAL AND METHODS

The material required for the auger picks was selected as 41Cr4. The chemical composition of the alloy is given in Table 1. The mechanical properties of this material are density 7834 kg/m³, yield strength 1032.18 MPa, Poisson's ratio 0.283 (Table 2). While designing the moulds of the pick to be shaped, the models were designed using the “indent” command in the SolidWorks program.

Table 1. Chemical content of the alloy (w.%)

C (%)	Si (%)	Mn (%)	P _{max} (%)	S _{max} (%)	Cr (%)
0.38-0.45	0.15-0.40	0.60-0.90	0.035	0.035	0.90-1.20

Table 2. Mechanical properties of the 41Cr4 alloy

Yield Stress (0.2%) [MPa]	Poisson rate	Density [kg/m ³]	Effective Plastic Strain	Deformation Rate, [1/s]
1032.18	0.238	7834 kg/m ³	0.05 Min 0.8 Max	0.01 Min 40.0 Max

During the mould design, the aggregate connection size of the 09-32CAT Tamping tool machine, one of the railway machines, was taken as a basis. Closed forging moulds were prepared for the body and shoveling part for the pick forging operations. While the connection and body parts of the pick were formed in the first mould, the shoveling part was planned to be shaped in the second mould. The diameter of the aggregate connection part of the pickaxe is 70 mm, the width of the shoveling part is 120 mm, the shoveling (mixer) part is 80 mm, and the length (including the shoveling part) is designed and modelled as 502 mm (Fig.1).

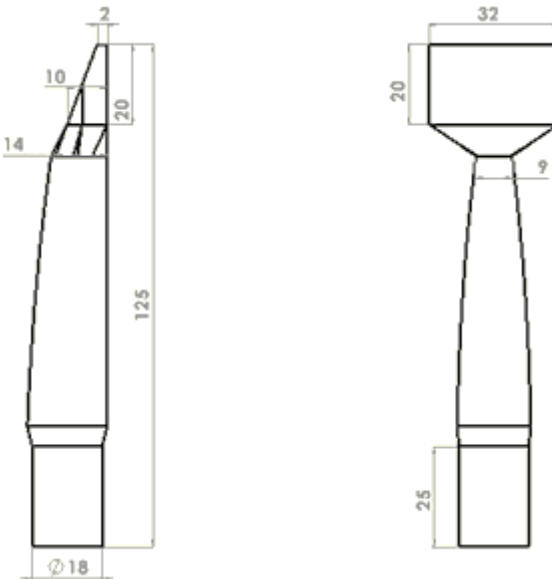


Fig. 1. Dimensions of the auger excavation

When drawing the pickaxe, the body work for high strength and an ellipsoid design has been made according to the direction of rotation, and the angles required to remove the mould are also given. For this reason, the moulds were removed by assigning a new plane while drawing in the indent command. In addition, a 5 mm radius was

given to all edges to avoid sharp corners and edges in the mould. In the modelled moulds, in order to distribute the load of the mould equally in all directions, the model was renewed and improved with continuous feedback by considering the stresses in the design. In order to prevent shavings from damaging the mould and press during shaping, the burr cavities were made at an angle according to the part where the material will be placed, and the modelling was completed by making sure that the material flow is homogeneous and linear. The workpiece will be shaped in the digging moulds in Figures 2 and 3, and the clamping and body part will be formed. At this stage, it will be shaped in the shovelling part, and another mould is required to give it its full form. The position of the workpiece in the mould is of great importance for the workpiece to fill the mould and to minimize the formation of burrs.

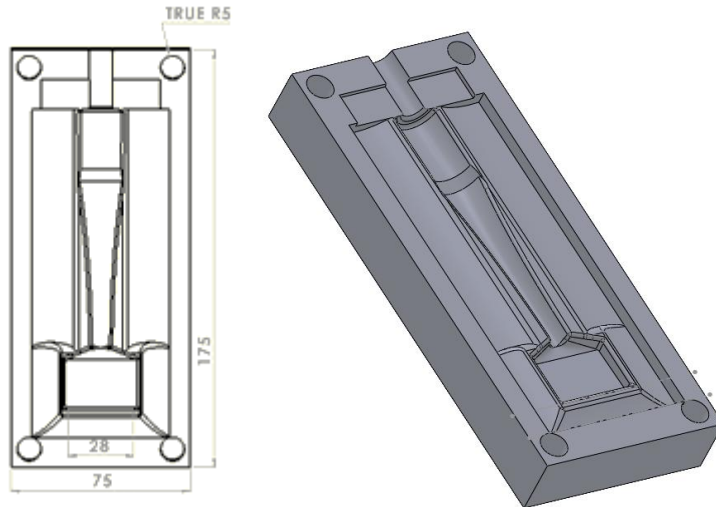


Fig. 2. Upper mould modelled for the body and clamping part

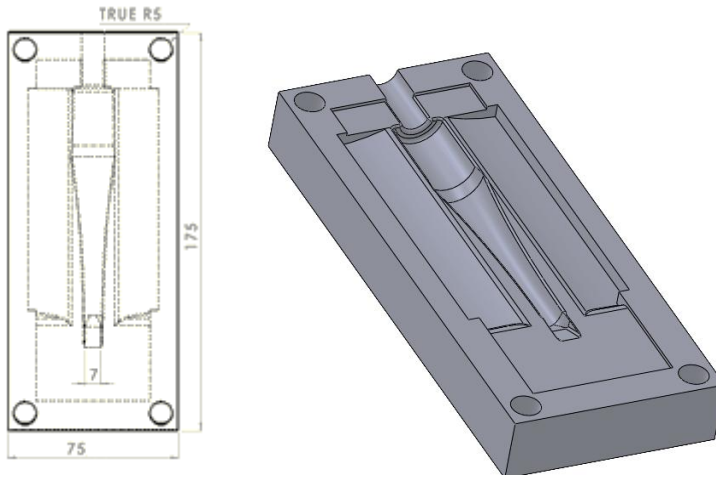


Fig. 3. Lower mould modelled for the body and clamping part

After the modelling, the location of the workpiece was optimized in the analyses, and information about its final position was obtained. The workpiece with the clamping and body part should be placed in a second mould to form the spherical part without losing its temperature (Figure 4).

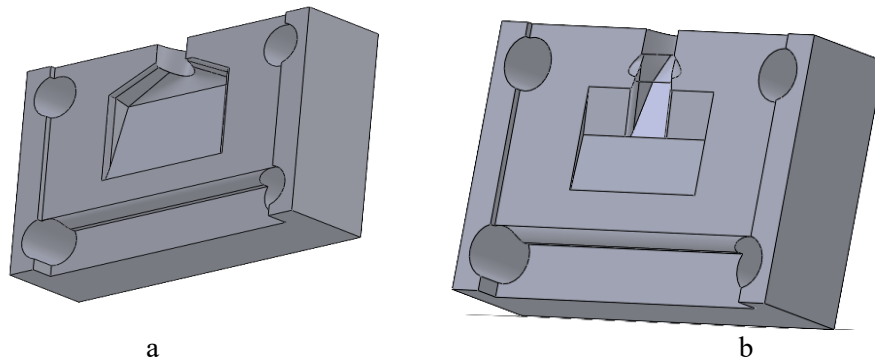


Fig. 4. a) upper, b) lower moulds required for shaping the plough section.

After the forging process is completed in the completely forged workpiece, the workpiece will be taken directly out of the mould and taken to the spherizing moulds for shaping the spherizing part. No heat treatment was applied to the material during the workpiece transfer between the moulds. When the forging operations were completed, the material was removed from the mould, burr cutting was performed, and forging was performed again for the ploughing part.

Finite Element Analysis (FEA)

41Cr4 alloy material was used for material selection during the analysis (Table 2). Density 7834 kg/m³, yield strength 1032.18 MPa, Poisson's ratio 0.283 were used in FEA. When placing the workpiece in the forging moulds, the temperature of 600°C for the workpiece was based on the ambient temperature of 20 °C (Fig. 7-8), and temperature optimization was also performed. The melting temperature of 41Cr4 steel is 1570 °C, which is below the soft annealing temperature of 600 °C selected for the process temperature. Considering that the sample required for the auger excavation, the dimensions of which are given in Figure 1, will be obtained by casting, the required dimensions were optimized and shown in Figure 5. For the experimental conditions, the dimensions of the workpieces were reduced by 1/4 and used in the FE analysis.

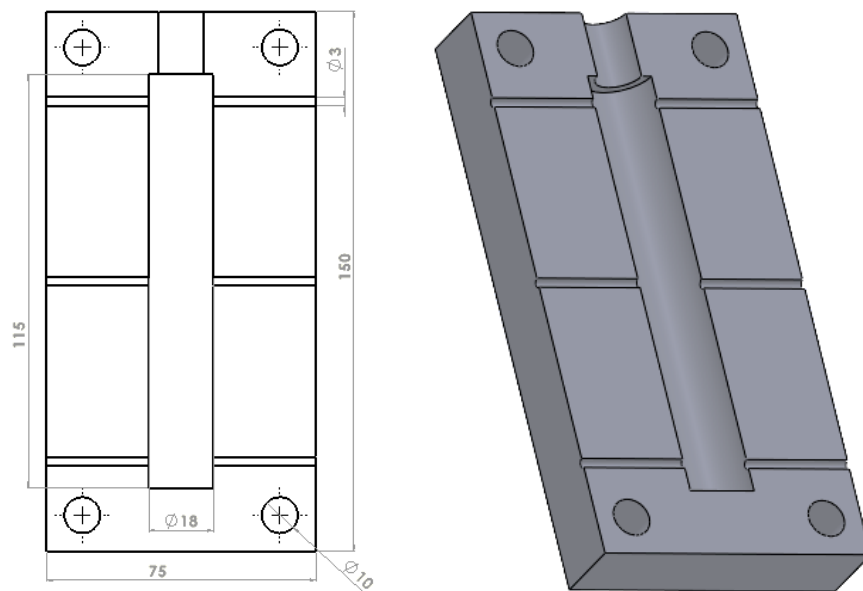


Fig. 5. Reduction of workpiece dimensions and casting mould by 1/4

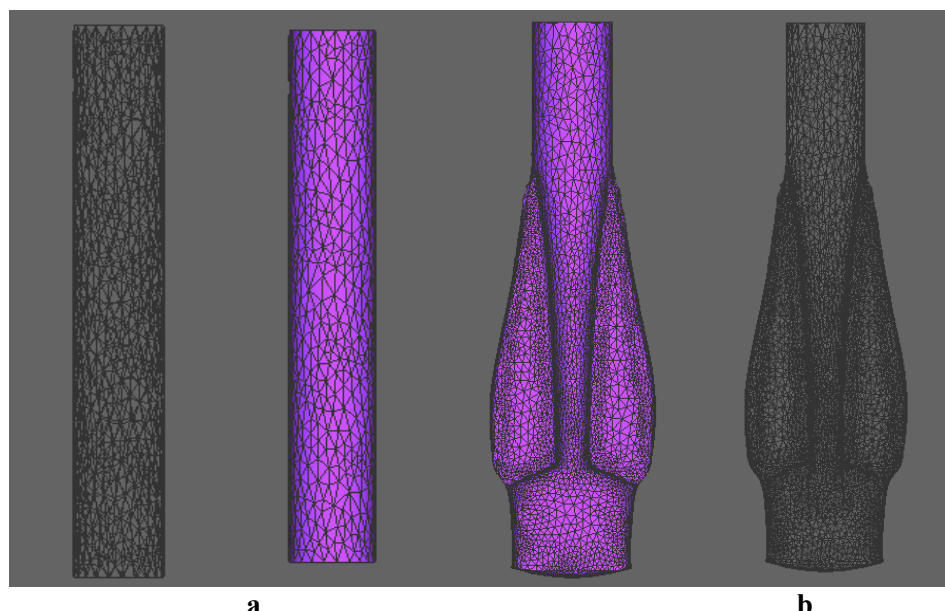


Fig. 6. Workpiece mesh a) for the untreated workpiece body and clamping part, b) Mesh example of the workpiece to be used in the ploughing part

3. RESULTS AND DISCUSSION

3.1. FE Analysis of Main Body and Connection Part

It is of great importance to know the pressing force to be applied while shaping the workpiece. For this reason, the pressing force under which the FEA modelled part will be shaped is determined by using the force time graphs obtained in Simufact program.

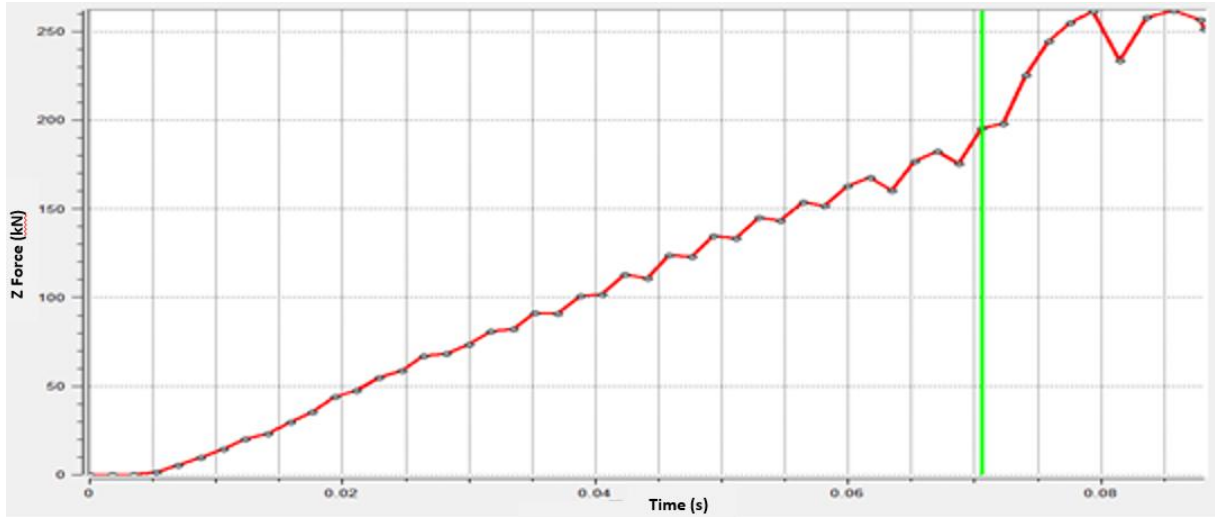


Fig. 7. Force-time graph of body and binding shaping.

In Figure 8, the maximum pressing force was determined as 250 MPa. A continuously increasing force-time graph is seen, and it is very valuable in terms of understanding whether the mould is pressing the burr or not. Up to 200 MPa, the pressing force increased proportionally, and after 82% deformation, the slope changed and increased to 50 MPa. At this point, the efficiency of the flow and the presence of problems such as burrs can be suspected. However, since it would not be correct to evaluate alone, it is necessary to look at the stress and strain values at different deformation values. It was observed that the highest equivalent stress was approximately 704.56 MPa in pressing operations performed at 30% feed rate, 638.13 MPa at 50% feed rate, and 611.55 MPa at 70% feed rate.

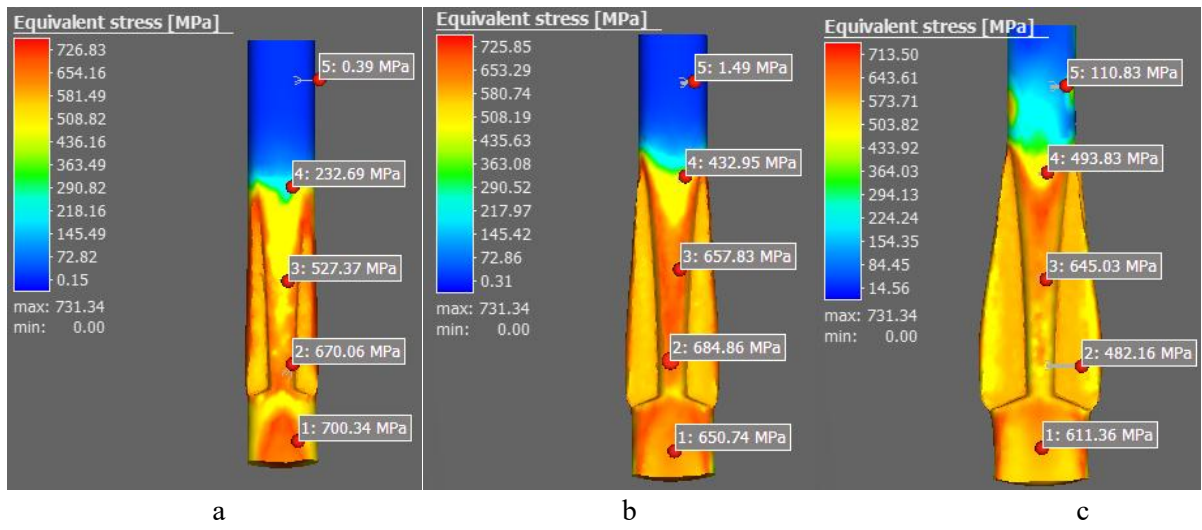


Fig. 8. Equivalent stresses at a) 30% b) 50% c) 70% deformation value

It is seen that the highest stress is observed in the spherical part of the material and in the connection part of the sphere and the body. It is seen that the equivalent stress decreases as the progress percentage increases in the remaining parts of the sample, except the connection part, and increases in the connection part (Figure 8).

It is seen that the highest effective plastic strain is 0.35 at 30% feed rate, 0.66 at 50% feed rate, and 0.91 at 70% feed rate, and the strain distribution is similar at all feed rates. In this case, with the pressing force applied, the material first filled the mould, and the excess material overflowed into the burr channels (Figure 9). In the FE

analysis started at 600 °C, as the deformation rate increases, cooling occurs in the parts of the workpiece in contact with the mould, while the temperature increases in the body part (Figure 10). In the analysis started at 600 °C, it was observed that the maximum temperature reached up to 876 °C in the body part of the workpiece. In the body and spherical part of the workpiece, a temperature change of ± 50 °C was observed (Figure 10).

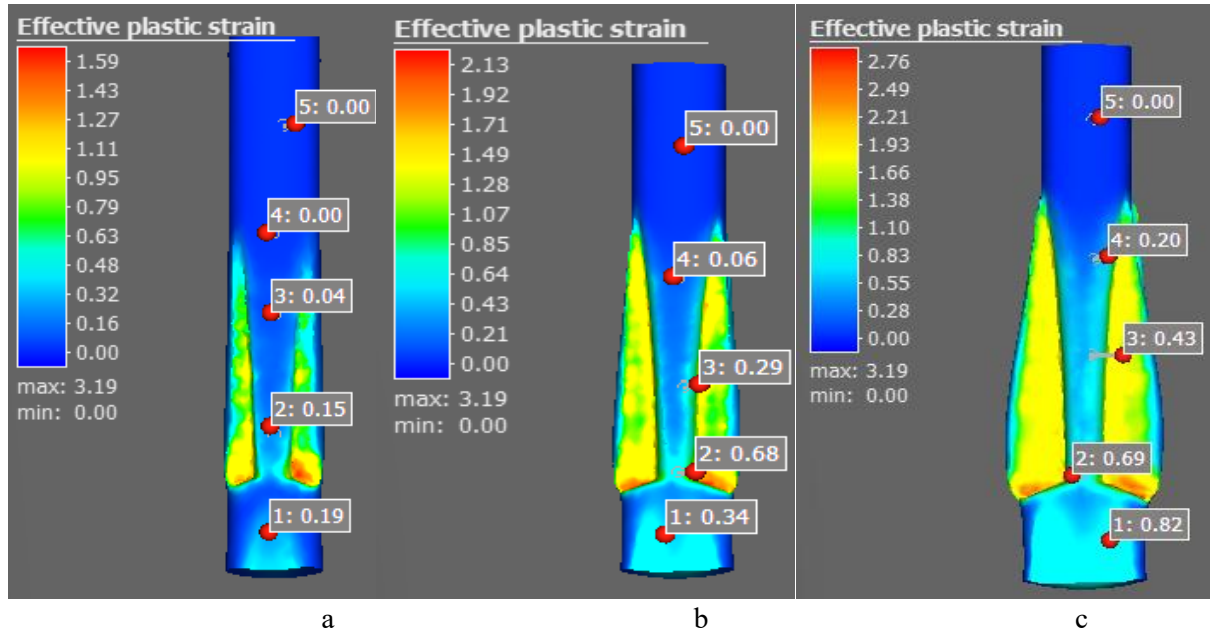


Fig. 9. Effective plastic strains at a) 30% b) 50% c) 70% deformation value

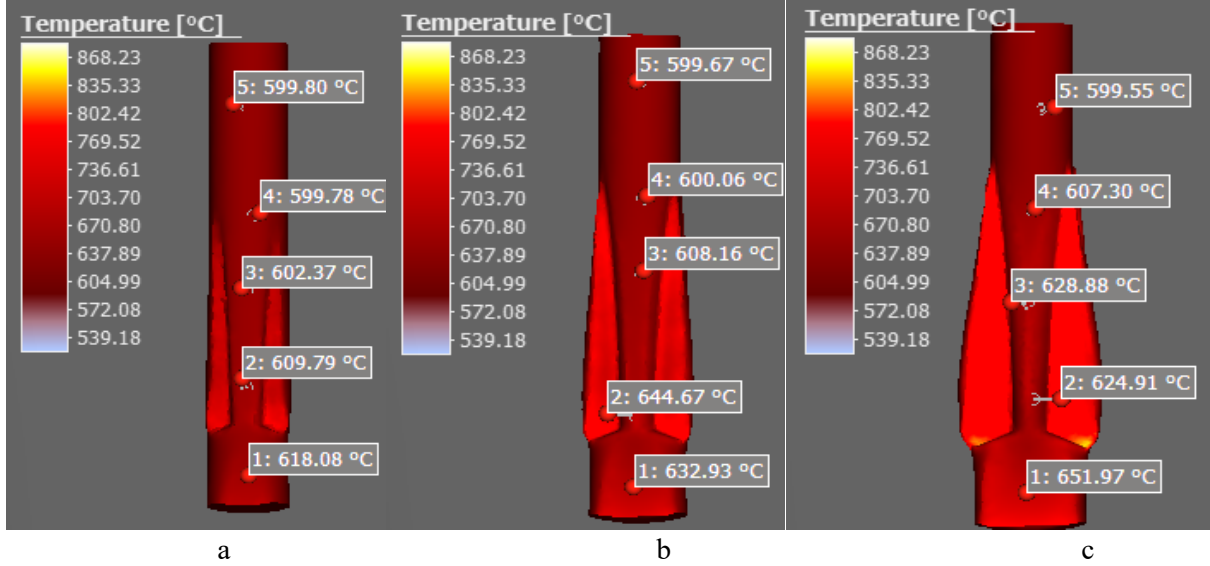


Fig. 10. Temperature changes at a) 30% b) 50% c) 70% deformation value.

The study of material flow is of great importance for the shaping of the workpiece. Homogeneous or, in other words, laminar flow means that the workpiece can easily fill the mould to the narrowest edge corners, while a turbulent flow means that the workpiece can move unstably during pressing. According to the deformation ratios, the material flow values were observed at 30% deformation with 246 mm/s in the spherizing part, at 50% deformation with 213 mm/s in the body connection part, and at 70% deformation with 271 mm/s with the burr advancing into the burr cavity (Figure 11).

According to these values and based on the flow arrows obtained from Figure 11, laminar flow occurs and this flow shows that the material can be easily shaped in the mould. The fact that the flow occurs in the burr region after 70% deformation shows that the mould does not press the burr.

In the design of the main body, it was found that the forming temperatures of the mold and the part are quite suitable for metal flow. In addition, hot plastic forming is also suitable for forming high strength in the internal structure of the metal by deformation without changing the microstructure. While the stresses accumulated mainly at the edges and corners of the mold, these stresses were eliminated with the superior mold design.

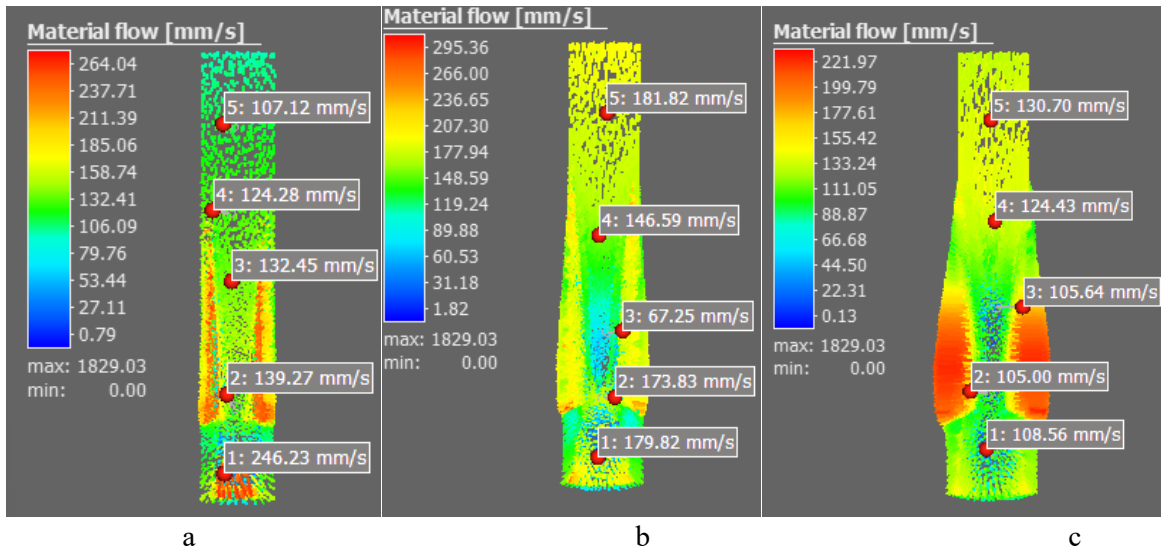


Fig. 11. a) 30% b) 50% c) 70% metal flow occurring at deformation values

3.2. FEA of The Moulding 2th Part

After the main body was shaped, the workpiece was removed from the mould and placed in the spherical moulds. This process was carried out by FE analysis. The results obtained from the previous FE analysis were transferred exactly to the mould in which the spherical part would be shaped, thus a more realistic FE analysis was performed.

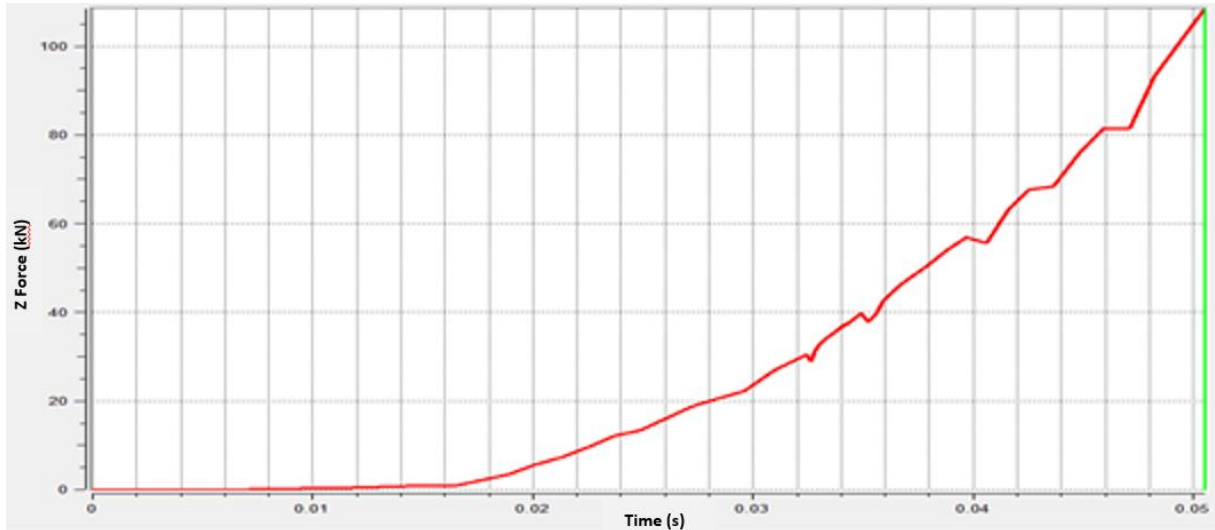


Fig. 12. Shovelling section Force-Time graph

As shown in Figure 12, the maximum pressing force was found to be 150 MPa, which is lower than the main body pressing force. It is seen that there is a linear relationship between the forming of the workpiece and the pressing force, and it is determined that the pressing forces are within acceptable limits, and it is also seen that the mould does not burr. Up to 80 MPa, the pressing force increased proportionally, and after 75% deformation, the slope changed and increased by 70 MPa and reaching 150 MPa.

It was observed that the highest equivalent stress at 30% deformation value was approximately 550 MPa at the upper edge of the sphere; this value was 591.95 MPa at the end of the sphere at 50% progression, and 615.86 MPa at the junction of the sphere and the body at 70% progression. It is seen that the highest stress is at the connection point of the sphere and the body at 70% deformation. As the deformation rate increases, it is seen that the equivalent stresses are very close to each other at every point of the workpiece and are lower than the body clamping part (Figure 13).

It is seen that the highest effective plastic strain in the pressing process performed as a result of 30% deformation is 1.00, 1.26 at 50% and 1.88 at 70%. In this case, with the pressing force applied, the material first filled the mould, and the excess material did not play a role in increasing the pressing force by moving towards the burr channels. In addition, the effective plastic strain in the moulding part occurred at the end of the moulding area where the metal flow was the highest, because the metal flow was higher in this part (Figure 14).

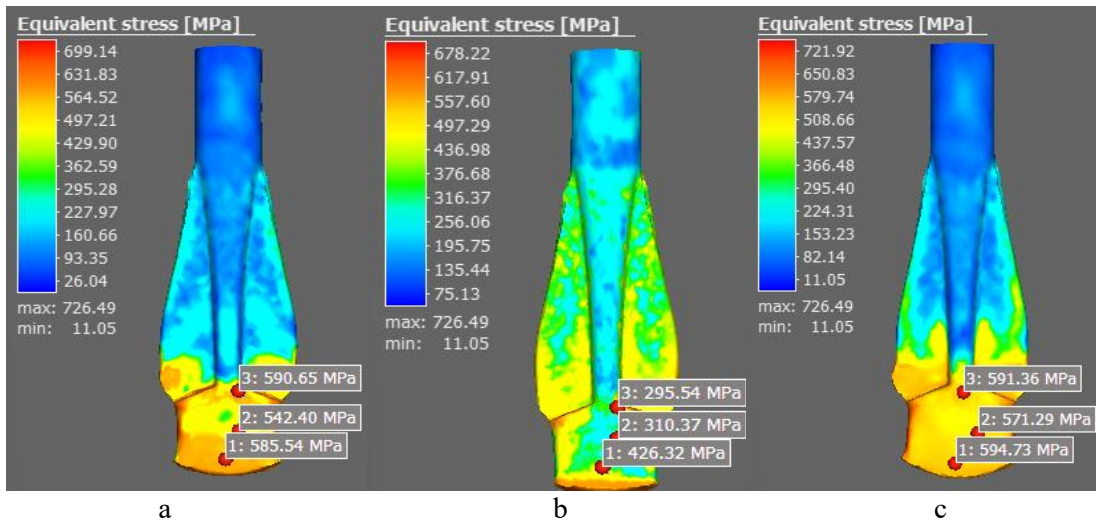


Fig. 13. Equivalent stresses occurring at a) 30% b) 50% c) 70% deformation values in the ploughing mould

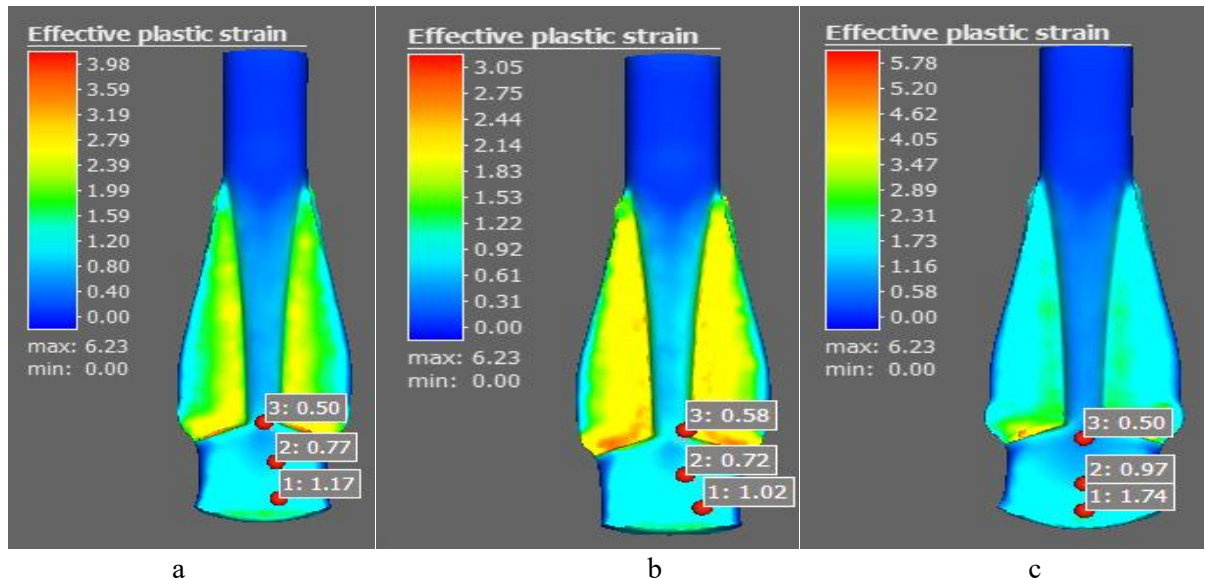


Fig. 14. Effective plastic strains occurring at a) 30% b) 50% c) 70% deformation values in the ploughing mould.

The temperature value decreased slightly due to the pressing of the body and started at 560 °C, and it was observed that this temperature increased to 985 °C with the shaping of the sphere part. However, this temperature value is the value remaining from the previous process, and the value occurring in the spheroid part was measured at a maximum value of 687 °C and 30% deformation value (Figure 15).

In the analysis started at 600 °C, it was observed that the maximum temperature reached up to 687 °C in the spherical part of the workpiece.

In Figure 15, which shows the material flow of the workpiece, the highest flow occurred in the body part with 31-350 mm/s, and this value is due to the backward movement of the paddle part during shaping. Initially, the flow rate was 135.56 mm/s during 10% deformation. While the workpiece in the mould was taking its final shape, the flow rate was 118.25 mm/s during 30% deformation and as the workpiece was shaped, the flow rate decreased gradually and was recorded as 83.25 mm/s at 70% deformation. Generally, the flow was laminar with no folds or overflow out of the mould.

The FEA results show that the designed molds prevent wrinkles, which is one of the major problems in open die production. The metal flow in the main body, which was molded at 600 °C without reaching high temperatures, was proof that it was designed to fill all the curves of the mold at the desired speed. In addition, the shovel part was redesigned to better penetrate the soil, and the desired shape was achieved with an open mold. With the two-step process, which is our main purpose, the tamping tool could be molded.

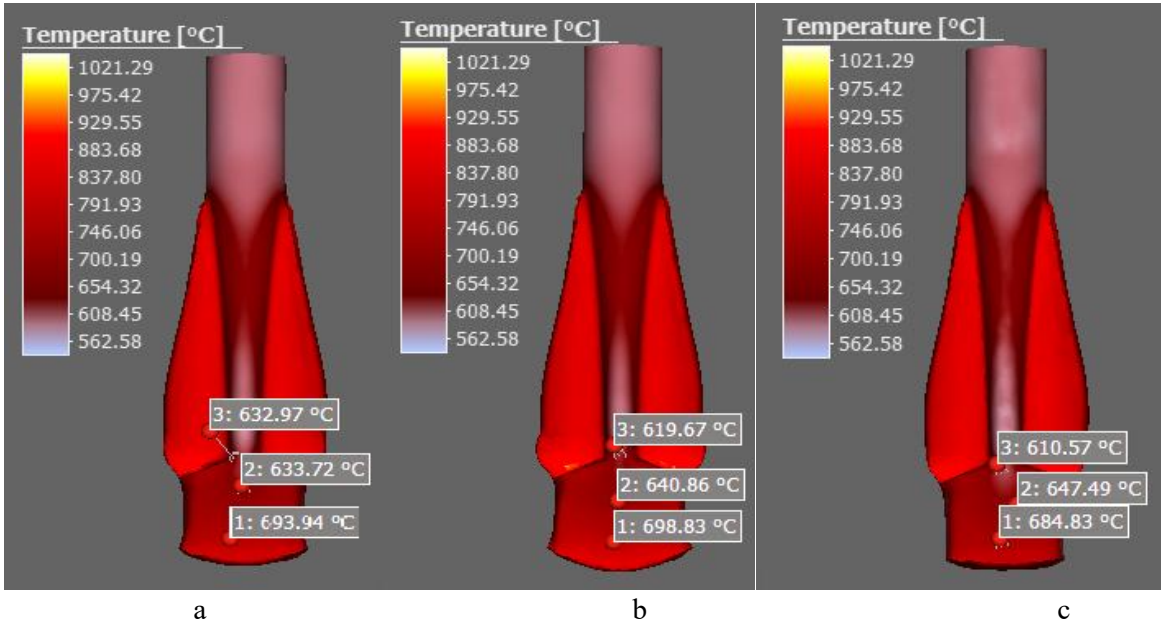


Fig. 15. Temperature changes occurring at a) 30% b) 50% c) 70% deformation value in the spherical mould

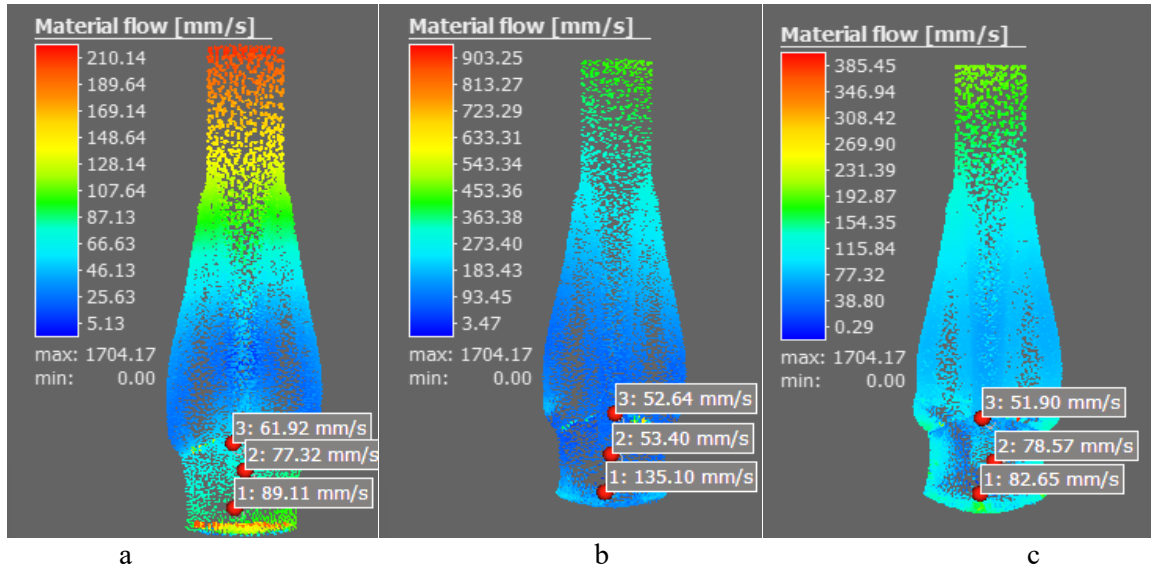


Fig. 16. Metal flow occurring at a) 30% b) 50% c) 70% deformation values in the ploughing mould

4. CONCLUSIONS

FE analyses were performed on the workpiece in the body clamp and blade dies designed to produce auger picks, and the analyses were carried out using 41Cr4 steel. The press force was reduced by minimizing the frictional force and the maximum press force was found to be 200 tons, and maximum stress values occurring during the forming of the workpiece were found to be 721 MPa, and the strains were found to be 5.78. The workpiece exhibited laminar flow in the die, and the maximum flow rate was recorded as 903 mm/s. No folding or cracking was detected during metal flow analysis. In the closed die pressing process conducted at 600 °C, the temperature of the workpiece was observed to rise to 1021 °C instantaneously, and it was concluded that it could not affect the microstructure as it did not remain at this temperature for a long time. The tamping tool, usually produced in at least 3 or 4 steps, could be produced in two steps. From all the FE analyses, it can be seen that 41Cr4 steel can be produced effectively by closed die pressing.

Author contributions: Conceptualization, design of the paper, supervision, review and editing, funding acquisition, L.P-P; conceptualization, supervision, validation, D.M-C; data curation, methodology, investigation, initial draft writing M.D.S-C; data curation, methodology, investigation, initial draft writing, J.S.R-H.; data curation, methodology, investigation, initial draft writing, P.U.L-G; All authors have read and agreed to the published version of the manuscript.

Funding source: This study has been supported by the Scientific Research Projects Management System of the Atatürk University (BAP- FYL-2024-13972).

Conflicts of interest: There is no conflict of interest.

REFERENCES

[1] Y. Çati, S. Gökçeli, Ö. Anil, C. Ş. Korkmaz, (2021), *Railway Engineering Development of a Numerical Model for the Analysis of the Effect of Under Sleeper Pad (Tap) Component on the Vibration Behavior of Rail, Sleeper and Ballast Components*, Dergipark, 14, 1-8, Doi: 10.47072/Demiryolu.

[2] A. Ulu, (2016), *Analysis of Railway Superstructure Vibrations under Live Load Effect*, Master Thesis. Yıldız Technical University, Department of Mechanical Engineering, İstanbul.

[3] M. Demirdağ, (2024), *Line Maintenance and Cost in Urban Rail Systems*, Accessed: Dec. 01, 2024. [Online]. <https://Polen.İtu.Edu.Tr/Bitstreams/3bc8c747-3086-4d4f-B247-E01c6d20f235/Download>

[4] Ersin Çakır, (2014), *Experimental Investigation of Tribological Properties of Plain Bearings Used in Aggregate Unit of Railways Burage Machines*, Master Thesis. Süleyman Demirel University, Isparta.

[5] S. Jovanovic, H. Guler, (2005), *Preliminary Required Works Before increasing the speeds On Railways*, Available: <https://Www.Researchgate.Net/Publication/293781839>

[6] Bilgehan Doğan, (2011), *Investigation of the Usability of AISI 1040 and AISI 4140 Steels Instead of AISI 1350 Steel Manufactured Buring Machine Picks*, Master Thesis, Cumhuriyet University Institute of Science and Technology.

[7] O. Barbir, D. Adam, F. Kopf, J. Pistrol, B. Antony, F. Auer, (2021), *In-Situ ballast condition assessment by tamping machine integrated measurement system*, IOP Conference Series: Earth and Environmental Science, IOP Publishing Ltd, 710, pp.12021, Doi: 10.1088/1755-1315/710/1/012071.

[8] H. C. Ji, R. Zhang, N. Z. Kang, J. H. Huang, (2025), *Simulation Analysis Of Wheel Bearing forging process based on Deform*, Metalurgija, 64(1–2), 87–90.

[9] K. Shinozaki and K. Miyamoto, (2019), *Forging*, CRC Press, doi: 10.1201/9781351045636-140000415.

[10] L. Dudkiewicz, M. R. Hawryluk, T. Szymanska, S. Polak, J. Ziembka, Z. Gronostajski, (2024), *Application Of Numerical simulations for A Multivariant analysis Of The construction Of Tools Assigned for Hot Precision forging Of Small Size forging multiple systems*, Archives of Metallurgy and Materials, 69(3), 1215–1229, doi: 10.24425/Amm.2024.150945.

[11] S. Joshy, K. R. Jayadevan, M. S. George, B. Prasad, (2022), *Influence of Hot Forging on Microstructure In Double tempered H11 Hot Forging dies*, Metallurgical Research & Technology, 119(1), doi: 10.1051/Metal/2022004.

[12] T. Balan, E. Becker, L. Langlois, R. Bigot, (2017), *A New route for Semi-Solid steel forging*, Cirp Annals-Manufacturing Technology, 66(1), 297–300, doi: 10.1016/J.Cirp.2017.04.111.

[13] Y. Y. Yu, J. Zottis, M. Wolfgarten, G. Hirt, (2019), *Investigation Of Applying protective sheet Metal Die covers for Hot Forging dies On A Cross-Forging geometry*, International Journal of Advanced Manufacturing Technology, 102(1–4), 999–1007, doi: 10.1007/S00170-018-03250-4.

[14] A. Gontarz *et Al.*, (2021), *Forging of Mg-Al-Zn magnesium alloys On Screw press and forging hammer*, Materials, 14(1), doi: 10.3390/Ma14010032.

[15] Y. Hedicke-Claus, M. Kriwall, M. Stonis, B. A. Behrens, (2023), *Auto mated design Of Multi-Stage forging sequences for die forging*, Production Engineering-Research and Development, 17(5), 689–701, doi: 10.1007/S11740-023-01190-X.

[16] R. Dindorf, P. Wos, (2020), *Energy-Saving Hot Open Die forging process Of Heavy Steel Forgings On An Industrial hydraulic forging press*, Energies (Basel), 13(7), doi: 10.3390/En13071620.

[17] Miao Wan, Y.C. Lin, Ning-Fu Zeng, Ming-Song Chen, Chao Li, Xiao-Dong Zhan, Gui-Cheng Wu, Song Zhang, (2025), *Perception and reconstruction Of Temperature field in Forgings based On Physical Model and CNN Model*, Measurement, 242, doi: 10.1016/J.Measurement.2024.116210.

[18] V. M. Imayev, D. M. Trofimov, R. M. Imayev, (2025), *Microstructure, Mechanical properties and oxidation resistance of B-Solidifying TiAl based alloys*, Intermetallics (Barking), 176, doi: 10.1016/J.İnternet.2024.108556.

[19] A. Gontarz, Z. Pater, K. Drozdowski, (2013), *Hammer Forging Process Of Lever Drop Forging From Az31 Magnesium Alloy*, Metalurgija, 52(3), 359–362.

[20] J. W. Brooks, (2000), *Forging of Superalloys*, Mater Des, 21(4), 297–303, doi: 10.1016/S0261-3069(99)00069-2.

[21] S. A. McKelvey, A. Fatemi, (2012), *Surface finish effect On Fatigue behavior Of Forged steel*, Int J Fatigue, 36(1), 130–145, doi: 10.1016/J.Ijfatigue.2011.08.008.